ISSN (Print) : 2320 – 3765
ISSN (Online): 2278 – 8875

International Journal of Advanced Research in Electrical, Electronics and Instrumentation Engineering

(An ISO 3297: 2007 Certified Organization)

Vol. 3, Issue 9, September 2014

DC-DC Converter with Coupled-Inductor For Multiple-Outputs

Pulla Sravani Kumari [1], Kasthuri Gunavardhan[2]

M.Tech Scholar, Department of EEE, SITAMS, Chittoor, Andhra Pradesh, India[1]

Professor, Department of EEE, SITAMS, Chittoor, Andhra Pradesh, India [2]

ABSTRACT: In this paper, the design methodologies are used to obtain the multiple outputs of DC-DC converter with a coupled inductor. The proposed system consists of single input of low voltage level, which can be boost into two different voltage levels. In this topology a coupled inductor with only one power switch is utilized for voltage clamping and soft switching operation. The two output voltages in this topology are obtained by limited components. The output voltages obtained are middle voltage and high voltage terminals are taken as power for a dc load applications. This topology is developed for high efficiency power conversion and two different voltages for dc loads. The proportional-integral derivative (PID) controller is designed in DC-DC converter to reduce the rise time and steady state error, and is modelled using SIMULINK and simulation results are obtained. It is referred as single input multiple output DC-DC converter.

KEYWORDS: Coupled inductor, high-efficiency power conversion, single-input multiple-output (SIMO) converter, soft switching, voltage clamping.

I.INTRODUCTION

In recent years the demand of energy is growing, rising the public awareness for environment. To protect the earth from global warming, created demand for the development of clean energy without pollution, have resulted in much of the research work focused on clean energies, such as fuel cell (FC), photovoltaic, and wind energy, etc., Because of the electric characteristics of clean energy, the generated power is critically affected by the climate or slow the transient responses, and the output voltage by load variations are easily influenced [1]-[3]. To ensure the proper operation of clean energy, other auxiliary components, e.g., storage elements, control boards, etc., are usually required. The fuel cell generation is one of the most efficient solutions for environmental pollution. In general various DC-DC converters with different voltage gains are made to satisfy the requirement of different voltage levels, so that the system control is complicated and corresponding cost is more expensive [4]. Here the conventional SIMO DC-DC converter capable of generating buck, boosts, and inverted outputs simultaneously. However, over three switches for one output were required. This scheme is suitable for only the low output voltage and power application, and its power conversion is degenerated because of hard switching operation.

Although a multi-output DC-DC converter shared zero-current-switching (ZCS) lagging leg having soft switching property can reduce the switching losses, but it is a three full-bridge converter scheme of more complicated. By this scheme the high-efficiency power conversion is difficult to achieve, and its cost is more expensive [5]-[6]. This paper presents a newly designed SIMO converter with a coupled inductor and uses one power switch to achieve its objectives of high-efficiency power conversion, high step-up ratio, and different and different voltage levels. In SIMO converter the utilisation of a low-voltage-rated power switch with small $R_{DS\ (on)}$, the soft switching techniques and voltage clamping are obtained to reduce the switching losses. The slew rate in the coupled inductor causes change in current it is restricted by leakage inductor [7]. The current transition time enables the power switch to turn ON with property of ZCS easily, and the effect of the leakage inductor can make less severe the losses caused by the reverse recovery current. The voltages of middle-voltage output terminals can be approximately adjusted by the design of auxiliary inductors and the high voltage DC bus can be stably controlled by a voltage proportional-integral derivative (PID) control. The section VI provides results to validate the effectiveness of the proposed SIMO converter and conclusions are drawn in section V.

ISSN (Print) : 2320 – 3765
ISSN (Online): 2278 – 8875

International Journal of Advanced Research in Electrical, Electronics and Instrumentation Engineering

(An ISO 3297: 2007 Certified Organization)

Vol. 3, Issue 9, September 2014

II. CONVERTER DESIGN AND ANALYSIS

The proposed system consists of high-efficiency SIMO converter topology to generate two different voltage levels from a single-input power source is depicted in Fig. 1. This SIMO converter contains five parts in this topology a low-voltage-sides circuit (LVSC), a clamped circuit, a middle-voltage circuit, an auxiliary circuit, and a high-voltage-side circuit (HVSC). The major symbol representations are V_{FC} (i_{FC}) and V_{O1} (i_{O1}) denote the voltages (currents) of the input power source and the output load at the LVSC and the auxiliary circuit, respectively; V_{O2} and i_{O2} are the output voltages and current in the HVSC whereas C_{FC}, C_{O1}, and C_{O2} are the filter capacitors at the LVSC is the auxiliary circuit, and the HVSC, respectively; C_1 and C_2 are the clamped and middle-voltage capacitors in the clamped and middle-voltage circuits, respectively, Lp and Ls represent individual inductors in the primary and secondary sides of the coupled inductor Tr, respectively, where the primary side in connected to the input power source Laux is the auxiliary circuit inductor. The main switch is expressed as S_1 in the LVSC; the equivalent load in the auxiliary circuit is represented as RO_1 and the output load is represented as RO_2 in the HVSC. The corresponding equivalent circuits is given in Fig. B is used to define the voltage polarities and current directions. The coupled inductor in Fig. A can be modelled as an ideal transformer including the magnetizing inductor L_{mp} and the leakage inductor Lkp in Fig. B. The turns ratio N and coupling coefficient k of Fig. B Equivalent circuit. This ideal transformer defined as

$$N=N_2/N_1 \quad (1)$$

$$k=L_{mp}\,(L_{kp}+L_{mp})=L_{mp}/L_p \quad (2)$$

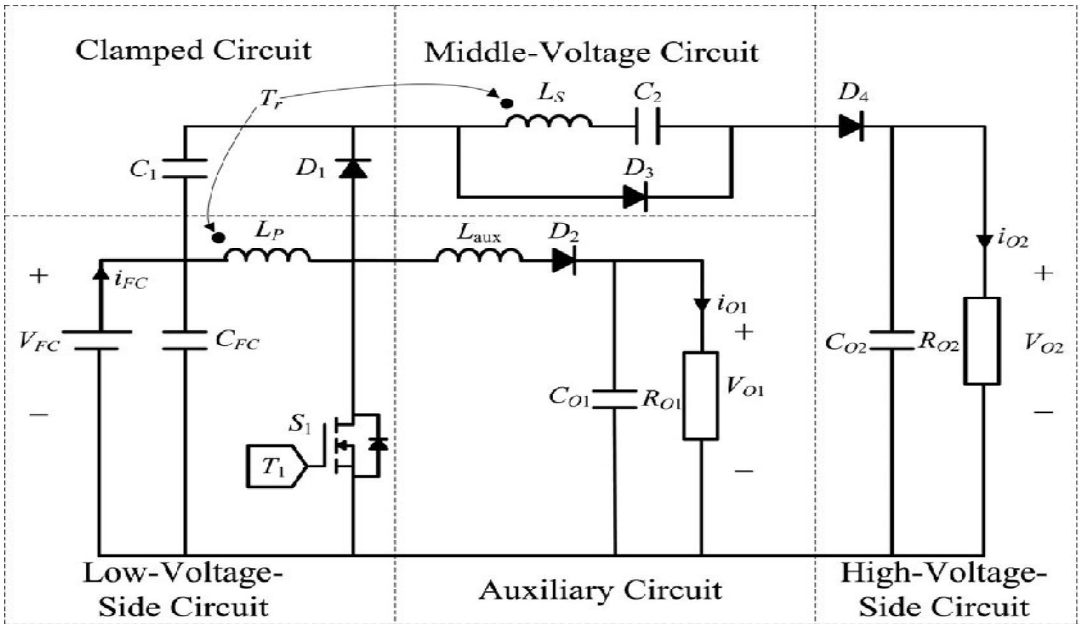

Fig. A. System configuration of high-efficiency single-input multiple-output (SIMO) converter

where N_1 and N_2 are the winding turns in the primary and secondary sides of the coupled inductor T_r. Because the voltage gain is less sensitive to the coupling coefficient and the clamped capacitor C_1 is approximately selected to completely absorb the leakage inductor energy, the coupling coefficient could be simply set at one (k=1) to obtain $L_{mp=}$ L_P via (2). In this study, the following assumptions are made to simplify the converter analyses: The main switch including its body diode is assumed as an ideal switching element; and the conduction voltage drops of both the switch and diode are neglected.

.

ISSN (Print) : 2320 – 3765
ISSN (Online): 2278 – 8875

International Journal of Advanced Research in Electrical, Electronics and Instrumentation Engineering

(An ISO 3297: 2007 Certified Organization)

Vol. 3, Issue 9, September 2014

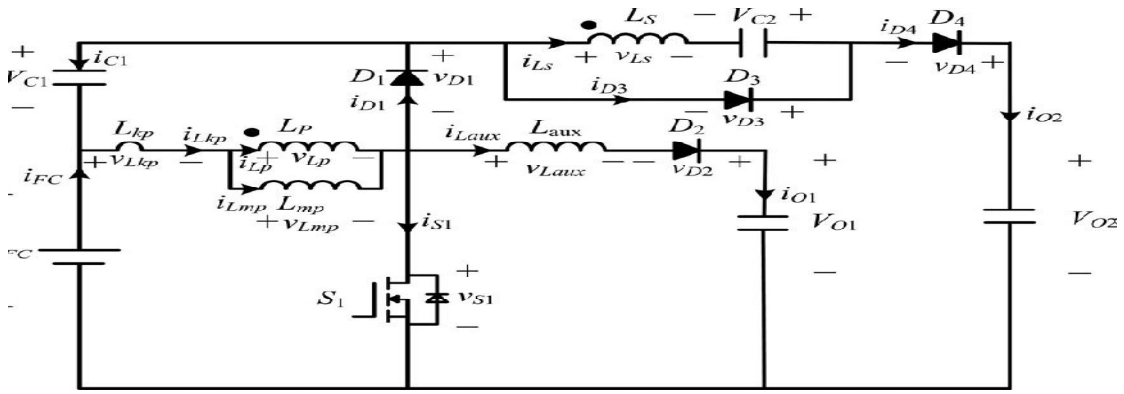

Fig. B. Equivalent circuit

III. OPERATION MODES

The characteristics waveforms are shown Fig. C and the topological modes in one switching cycles are illustrated in Fig.4.

Mode 1(t0—t1) [Fig (a)]: In this mode, the main switch S_1 was Turned ON for a span, and the diode D_4 Turned OFF. Because the polarity of the winding of the coupled inductor T_r is positive, the diode D_3 turns ON. The secondary Current i_{LS} reverses and charges to the middle voltage capacitor C_2.When auxiliary inductor Laux releases its stored energy completely, and the diode D_2 Turns off, this mode ends.

Mode 2 (t1−t2) [Fig (b)]: At time t =t1, the main switch S1 is persistently turned ON. Because the primary inductor L_P is charged by input power source, the magnetizing current i_{Lmp} increases gradually in an approximately linear way. At the same time, the secondary voltage V_{LS} charges the middle-voltage capacitor C_2 through the diode D_3.Athough the voltage V_{Lmp} is equal to the input voltage V_{FC} both at modes 1and 2, the ascendant slope of the leakage current of the coupled inductor (diLkp/dt) at modes1 and2 is different due to path of the auxiliary circuit. Because the auxiliary inductor L_{aux} releases its stored energy completely, and the diode turns OFF at the end of mode 1, it results in reduction of di_{Lkp}/dt at mode 2.

Mode 3 (t2—t) [Fig (c)]: At time t= t2, the main switch S1 is turned OFF. When the leakage energy still releas2ed from the secondary side of the coupled inductor, the diode D_3 persistently conducts and releases the leakage energy to the middle–voltage capacitor C_2. When the voltage across the main switch V_{S1} is higher than voltage across the clamped capacitor V_{C1}, the diode D_1 conducts to transmit the energy of the primary –side leakage inductor L_{kp} into the Clamped capacitor C_1.At the same time, partial energy of the primary-side leakage inductor L_{kp} is transmitted to the auxiliary inductor Laux, and the diode D_2 conducts. Thus, the current i_{Laux} passes through the diode D_2 to supply the Power for the output load in the auxiliary circuit. When the secondary side of the coupled inductor releases its leakage energy completely, and diode turns OFF, this mode ends.

Mode 4(t3—t4) [Fig (d)]: At the time t=t3, the main switch S_1 is persistently Turned OFF. When the leakage energy has released from the primary side of the coupled inductor, the secondary current i_{LS} is induced in reverse from the energy of magnetizing inductor L_{mp} through the ideal transformer, and flows through the diode D_4 to the HVSC. At the same time, partial energy of the primary side leakage inductor L_{kp} is still persistently transmitted to auxiliary inductor L_{aux}, and the diode D_2 keeps conducting. Moreover, the current iLaux passes through diode D_2 to supply the power for the output load in auxiliary circuit.

Mode 5 (t4— t5) [Fig (e)]: At time t=t4, the main switch S_1 is persistently turned OFF, and the clamped diode D_1 Turns OFF because the primary leakage current i_{Lkp} equals to auxiliary inductor current i_{Laux}. In this mode, the input power source, and the primary winding of the inductor T_r, and the auxiliary inductor L_{aux} connect in series to supply the power for the output load in the auxiliary circuit through the diode D_2, At the same time, winding of the input power

10.15662/ijareeie.2014.0309040

ISSN (Print) : 2320 – 3765
ISSN (Online): 2278 – 8875

International Journal of Advanced Research in Electrical, Electronics and Instrumentation Engineering

(An ISO 3297: 2007 Certified Organization)

Vol. 3, Issue 9, September 2014

source, the secondary coupled inductor Tr, the clamped capacitor C_1, and the middle-voltage capacitor (C_2) connect in series to release the energy into the HVSC through the diode D_4.

Mode 6(t5—t6) [Fig (f)]: At time t=t5, this mode begins when the main switch S1 is triggered. The auxiliary inductor Current i_{Laux} needs time to decay to zero, the diode D2 persistently conducts. In this mode, the input power source, the clamped capacitor C1, the secondary winding of the coupled inductor Tr, and the middle-voltage capacitor C2 still connect in series to release the energy into the HVSC through the diode D4. Since the clamped diode D1 can be selected as a low –voltage Schottky diode, it will be cut off promptly without a reverse current. Moreover, the rising rate of the primary current iLkp is limited by primary-side leakage inductor Lkp. Thus, one cannot derive any currents from the paths of the HVSC, the middle-voltage circuit, the auxiliary circuit, and the clamped circuit. As a result, the main switch

S1 is turned ON under the condition of ZCS and this soft-switching property is helpful for alleviating the switching loss. When the secondary current i_{LS} decays to zero, this mode ends. After that, it begins the next switching cycle and repeats the operation in mode 1.

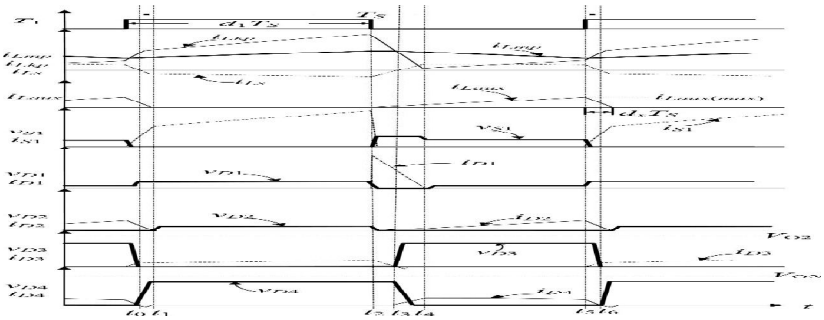

Fig. C. Characteristic waveforms of high-efficiency SIMO converter

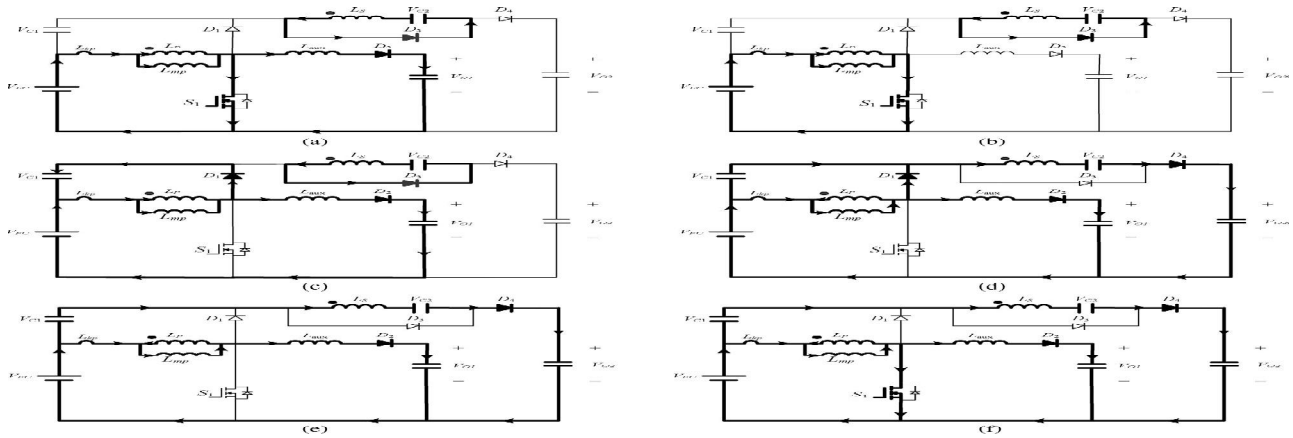

Topology modes: *(a)mode-1;(b)mode-2;(c)mode-3;(d)mode-4;(e)mode-5;(f)mode-6;*

Voltage Gain Derivation:

Here the magnetising inductor voltage v_{Lmp} is equal to the input power source V_{FC} at the mode 2, the voltage v_{Lmp} can be represented as

$$v_{Lmp} = V_{FC.} \quad (3)$$

Due to the relation of $v_{Ls}= Nv_{Lp} = VC_2$, the voltage VC_2 can be represented as

$$VC_2=NV_{FC}. \quad (4)$$

ISSN (Print) : 2320 – 3765
ISSN (Online): 2278 – 8875

International Journal of Advanced Research in Electrical, Electronics and Instrumentation Engineering

(An ISO 3297: 2007 Certified Organization)

Vol. 3, Issue 9, September 2014

By using the voltage-second balance, the relation of the average voltage across the magnetising inductor L_{mp} of coupled inductor Tr to be zero can be represented as

$$V_{FC}d_1Ts+v_{Lmp}(1-d1)\,Ts=0. \quad (5)$$

From (5), one can obtain $v_{Lmp} = [-d_1/(1-d_1)]\,V_{FC}$ (6)

Since the voltage of the clamped capacitor VC_1 is equal to the negative voltage of magnetising inductors voltage v_{Lmp} at modes 3 and 4, the voltage VC_1 can be expressed as (6)

$$VC_1=-v_{Lmp} = [d1/(1-d_1)]\,V_{FC.} \quad (7)$$

According to Kirchhoff's voltage law, the output voltage VO_2 can be obtained as

$$VO_2=V_{FC}+VC_1+VC_2-v_{Ls.} \quad (8)$$

By using the voltage-second balance, the relation of the average voltage across the secondary winding v_{Ls} to be zero, can be expressed by (4) and (8) as

$$(NV_{FC})\,d_1\,Ts + (V_{FC}+VC_1+VC_2-VO_2)\,(1-d_1)\,Ts=0 \quad (9)$$

From (4)-(9), the voltage gain G_{VH} of the proposed SIMO converter from the LVSV to the HVSC can be given as

$$G_{VH} = VO_2/V_{FC}=N+1/(1-d_1) \quad (10)$$

For calculating the discharge time of the auxiliary inductor at modes 1 and 6, the corresponding time interval can be denoted as d*x* Ts = [(t6-t5) + (t1-t0)]. By using the voltage-second balance, the relation of the average voltage across the auxiliary inductor L_{aux} to be zero can represented as

$$(V_{FC}-v_{Lmp}-VO1)\,(1-d_1)\,Ts+(-VO_1)\,dx\,Ts=0 \quad (11)$$

The voltage gain G_{VL} of the proposed SIMO converter from the LVSC to the auxiliary circuit can be obtained by (6) and (11) as

$$G_{VL} = VO_1/V_{FC}= 1/(1-d_1+dx) \quad (12)$$

Because the diode current i_{D2} is equal to the current iLaux, the average value of the diode current i_{D2} can be calculated.

$$i_{D2\,(avg)} = 1/Ts\,[1/2i_{Laux\,(max)}\,(1-d_1)Ts+1/2i_{Laux\,(max)}\,dx\,Ts] \quad (13)$$

Where Ts is the converter switching cycle, $i_{Laux\,(max)}$ is the maximum current of the auxiliary inductor and can be expressed as

$$i_{Laux\,(max)} = (VO_1/L_{aux})\,dx\,Ts. \quad (14)$$

By substituting (14) into (13), one can obtain $i_{D2\,(avg)} = VO_1/2\,L_{aux}\,dx\,Ts\,(1-d_1+dx)$ (15)

Because the average current of the diode D_2 is equal to the current iO_1, it yields

$$i_{D2\,(avg)} = VO1/RO1. \quad (16)$$

From (15) and (16), the duty cycle d*x* can be rewritten as

$$dx = -(1-d_1) + \sqrt{((1-d_1)^2+[8L_{aux}/RO_1Ts])}/2. \quad (17)$$

By substituting (17) into (12), the voltage gain G_{VL} of the proposed SIMO converter from the LVSC to the auxiliary circuit can be rearranged as $G_{VL}=VO_1/V_{FC}=2/[(1-d_1)+\sqrt{((1-d_1)^2+(8L_{aux}/RO_1Ts))}]$ (18)

ISSN (Print) : 2320 – 3765
ISSN (Online): 2278 – 8875

International Journal of Advanced Research in Electrical, Electronics and Instrumentation Engineering

(An ISO 3297: 2007 Certified Organization)

Vol. 3, Issue 9, September 2014

III. SIMULATION RESULTS

Here, the proposed converter can boost the 12volts of a low-voltage input power source to a controllable high-voltage 200volts dc bus and middle-voltage output 28volts terminals. The high-voltage dc bus can take as the main power for a high-voltage dc load or the front terminal of a dc–ac inverter. Moreover, middle-voltage output terminals can supply powers for individual middle-voltage dc loads or for charging auxiliary power sources (e.g., battery modules).

1. OPEN LOOP

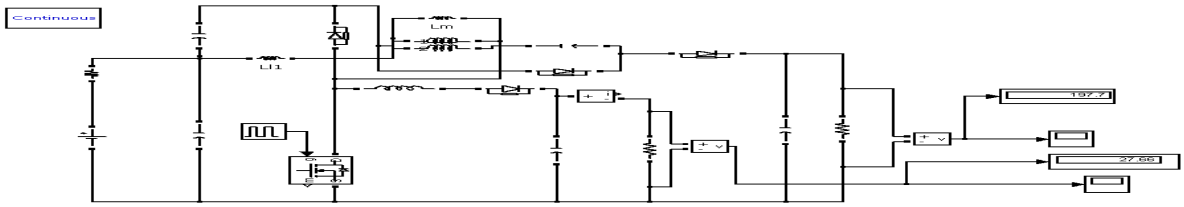

Fig.3. Open loop circuit of the proposed converter

The output voltages by above simulated circuit with single input of low voltage of 12V are obtained, two voltages of different levels as shown below. These voltages are obtained by the open loop circuit of SIMO converter shown below.

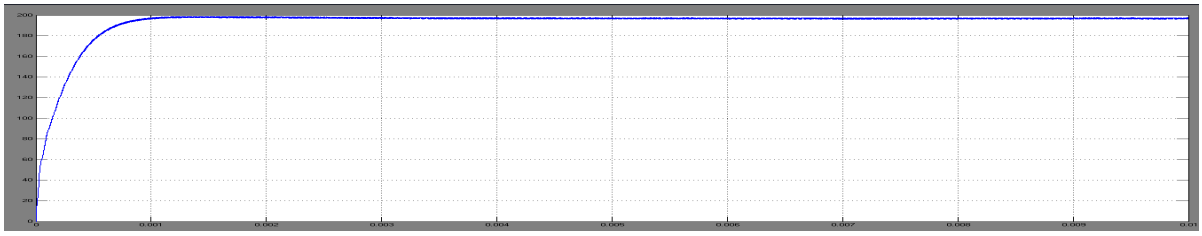

Fig.3.a. Output voltage of 200volts waveform of the SIMO converter, i.e. High DC voltage

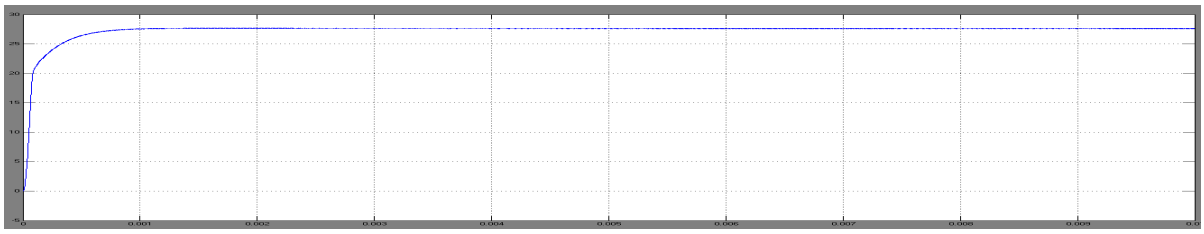

Fig.3.b. Output voltage 28volts waveform of the SIMO converter, i.e. auxiliary DC voltage.

2. CLOSED LOOP

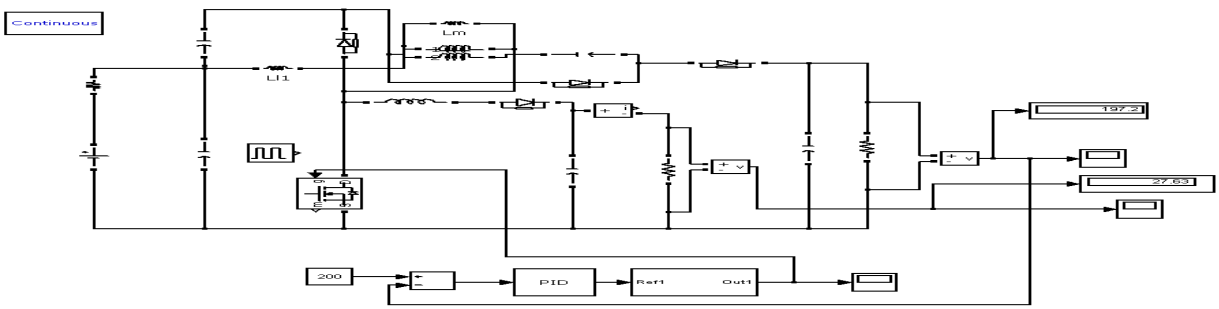

Fig.4. Closed Loop circuit of the proposed converter

ISSN (Print) : 2320 – 3765
ISSN (Online): 2278 – 8875

International Journal of Advanced Research in Electrical, Electronics and Instrumentation Engineering

(An ISO 3297: 2007 Certified Organization)

Vol. 3, Issue 9, September 2014

The above simulation cicuit is closed loop topology of SIMO converter, Here the input voltage is 12V and output voltages are of two difrerent levels are 200V and 28V obtained. Here PID controller is suggested to reduce the output voltage variations.

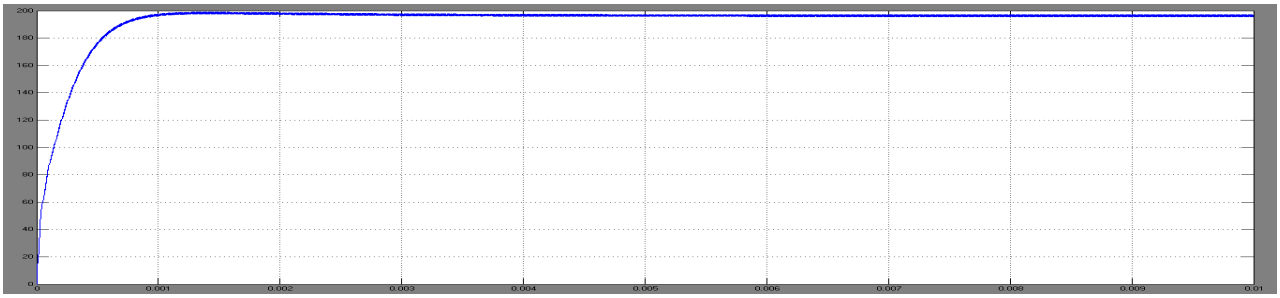

Fig.4.a. Output Voltage 200 volts waveform of the SIMO converter, i.e. high DC voltage.

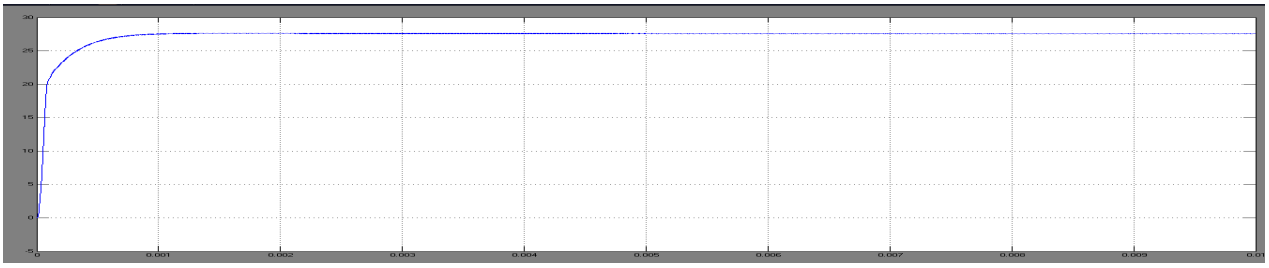

Fig.4.b. Output Voltage 28volts waveform of the SIMO converter, i.e. auxiliary voltage.

V. CONCLUSION

This paper has presented high-efficiency dc-dc converter, and this coupled-inductor-based converter was applied well to a single-input power source having two output terminals of an auxiliary battery module and a high-voltage dc bus. The results of SIMO converter is the maximum efficiency was measured to be exceed 95%, and the average conversion efficiency was measured over 91%.The proposed SIMO converter is suitable for the application such as one common ground, is preferred in most applications. The major scientific contributions of the SIMO converter are recited as follows:

1) This topology has only one power switch to achieve the objective of SIMO power conversion.
2) The voltage gain is substantially increased by using a coupled inductor
3) The stray energy is recycled by a clamped capacitor into the auxiliary battery module or high-voltage dc bus to ensure the property of voltage clamping.
4) An auxiliary inductor is providing the charge power to the auxiliary battery module and assisting the turned ON under the conditions of ZCS.
5) The switch voltage stress is not on the input voltage so that it is more suitable for a dc conversion mechanism with different input voltage levels.
6) The copper loss in the magnetic core can be greatly reduced, due to copper film with lower turns.

REFERENCES

1. Kirubakaran, S. Jain, and R. K. Nema, "DSP-controlled power electronic interface for fuel-cell-based distributed generation," *IEEE Trans. Power Electron.*, vol. 26, no. 12, pp. 3853–3864, Dec. 2011
2. M. Singh and A. Chandra, "Application of adaptive network-based fuzzy interference system for sensor less control of PMSG-based wind turbine with nonlinear-load-compensation capabilities," *IEEE Trans. Power Electron.*, vol. 26, no. 1, pp. 165–175, Jan. 2011

ISSN (Print) : 2320 – 3765
ISSN (Online): 2278 – 8875

International Journal of Advanced Research in Electrical, Electronics and Instrumentation Engineering

(An ISO 3297: 2007 Certified Organization)

Vol. 3, Issue 9, September 2014

3. S. D. Gamini Jayasinghe, D. Mahinda Vilathgamuwa, and U. K. Madawala, "Diode-clamped three-level inverter-based battery/ super capacitor direct integration scheme for renewable energy systems," *IEEE Trans. Power Electron.*, vol. 26, no. 6, pp. 3720–3729, Dec.2011
4. H.Wu, R. Chen, J. Zhang, Y. Xing, H. Hu, and H. Ge, "A family of three port half-bridge converters for a stand-alone renewable power system," *IEEE Trans. Power Electron.*, vol. 26, no. 9, pp. 2697–2706, Sep.2012.
5. F. Gao, B. Blunier, M. G. Sim˜oes, and A. Miraoui, "PEM fuel cell stack modelling for real-time emulation in hardware-in-the-loop application," *IEEE Trans. Energy Converters.*, vol. 26, no. 1, pp. 184–194, Mar. 2011. Y. Chen, Y. Kang, S. Nie, and X. Pei, "The multiple-output DC–DC converter with shared ZCS lagging leg," *IEEE Trans. Power Electron.*, vol. 26, no. 8, pp. 2278–2294, Aug. 2011
6. . Schuch, C. Rech, H. L. Hey, H. A. Gr¨undling, H. Pinheiro, and J. R. Pinheiro, "Analysis and design of a new high-efficiency bidirectional integrated ZVT PWM converter for DC-bus and battery-bank interface," *IEEE Trans. Ind. Appl.*, vol. 42, no. 5, pp. 1321–1332, Sep./Oct. 2006.
7. J. K. Kim, S.W. Choi, and G.W. Moon, "Zero-voltage switching post regulation scheme for multi output forward converter with synchronous switches," *IEEE Trans. Ind. Electron.*, vol. 58, no. 6, pp. 2378–2386,Jun. 2011.

BIOGRAPHY

PULLA SRAVANI KUMARI received B.Tech degree in Electrical and Electronic Engineering from Jawaharlal Nehru Technological University, Anatapur, India in 2011.Currently She is pursuing M.Tech, Power Electronics in Sreenivasa Institute of Technology and Management Studies, Chittoor, A.P, India. Her research interests are development in Power Electronics

KASTHURI GUNAVARDHAN Currently working as Professor in department of Electrical and Electronics Engineering, Sreenivasa Institute of Technology and Management Studies, Chittoor, A.P, India. His research interests include Power Electronics.